Embedded Radar Sensing in Communication Waveforms: Algorithms and Trade-off

Husheng Li

***Abstract*—Joint communication and sensing (JCS) is a promising technology that shares the same waveform for both the functions of communications and sensing, in order to improve the efficiencies of frequency spectrum and power. In this paper, the approach of reusing communication waveforms for sensing is studied. From the viewpoint of frequency domain, the communication signals provide bandwidth for radar ranging; from the viewpoint of time domain, the random information symbols in the communication signal offer timing information via the autocorrelation function. Both cases of single-carrier and multi-carrier communication signals are studied for embedding the sensing function. The trade-off between communication and sensing performances is studied.**

I. Introduction

Spectrum is a major fundamental resource for wireless technologies such as communications, radar, Internet of Things (IoT), radio astronomy, et al. Nowadays, wireless systems are facing the challenge of scarce spectrum resources. For example, substantial sub-6GHz bandwidth has been used by various applications, thus forcing the next generation (NextG) of wireless communications to exploit higher frequency band such as millimeter wave (mmWave), despite plenty of difficulties. Coexistence and resource sharing of different systems are efficient solutions to the challenge of spectrum scarcity.

In this paper, we will focus on the coexistence of communications and radar systems, and, in particular, go beyond the exclusive but dynamic frequency spectrum sharing, by sharing the same waveforms between data transmission and radar sensing. This is achieved by using the same radio frequency (RF) frontend and sending out a common waveform carrying both communication data packet (in the forward EM wave) and environmental information (in the reflected EM wave), thus unifying the two different systems into a common radio frequency (RF) platform called joint communications and sensing (JCS). This mechanism is illustrated in Fig. 1.

The waveform of JCS can be designed in three ways: radar waveform based, communication waveform based and dedicated waveform design. In this paper, we discuss the communication waveform based JCS. Compared with the dedicated waveform design, which needs numerical optimizations and extra hardware design, the communication waveform based JCS leverages existing designs and is thus easier for implementations; meanwhile, a significant shortage of the radar waveform based JCS is the low communication data rate (e.g., the data rate of information embedded in modulated frequency modulation continuous waveform (FMCW) radar is only in the order of 100kbps, as concluded by our experiment [22]). Therefore, the communication waveform based JCS is a good trade-off between feasibility and performance. We will consider both the single-carrier and multicarrier cases. The key challenge is how to realize the radar sensing function. In this paper, we will propose algorithms for radar sensing based on correlation analysis, which is computation-oriented, and time synchronization, which can be implemented in hardware and has been mature in existing communication systems [20]. Moreover, the trade-off between communications and radar sensing will also be analyzed, namely how the given frequency bandwidth serves both functions. Numerical results will show that *the same bandwidth is well shared by both communications and radar sensing, which implies that the conflict between communications and radar be marginal.*

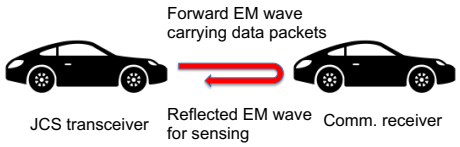

Fig. 1: Illustration of shared waveform in JCS

The remainder of this paper is organized as follows. The studies related to this paper are introduced in Section II. The signal model of JCS is explained in Section III. The performances of JCS with single and multiple carriers are discussed in Sections IV and V, respectively, based on which the trade-off between communications and sensing is analyzed in Section VI. Then, the numerical results are provided in Section VI. Finally the conclusions are drawn in Section VIII.

H. Li is with the Department of Electrical Engineering and Computer Science, the University of Tennessee, Knoxville, TN (email: husheng@eecs.utk.edu, phone number: 865-974-3861, fax number: 865-974-5483, address: 310 Ferris Hall, 1508 Middle Drive, Knoxville, TN, 37996).

II. Related Work

In the mmWave band, the communication signal can be used for localization based on different signal features [2]. In [3], the possibility of embedding sensing signals (e.g., as a preamble of OFDM symbol) to communications has been analyzed. In [4], the 60GHz radio signal is used for target tracking with high precision, which is similar to a bi-static radio system. The angle of arrival (AOA) of mmWave signals is studied in [5], [6], which can be used for the locationing of targets. Besides in communication systems, generic mmWave signal is also used in biometric sensing such as gesture [7], speech [8], RFID [9] and electronics devices [10]. Beyond the mmWave signal, other communication signal bands have been exploited for sensing. The Wi-Fi band has been intensively used for sensing various targets. Numerous sensing schemes leveraging Wi-Fi band signals have been proposed [11], [12]. Essentially, the sensing scheme using mmWave or Wi-Fi signals is similar to passive bistatic radars, in which the radar leverages other radiation sources (e.g., the mmWave communication signal) for almost free illuminations on the target and the corresponding sensing. The passive radio may also utilize the spontaneous radiation of the target itself [17], [18]. However, in these studies focusing on the algorithm designs, *the performance trade-off between communications and radar sensing is not analyzed for deepening the understanding of the JCS technology, thus leaving a pressing need for characterizing the conflict and balance between the two functions.* Meanwhile, none of the existing approaches have leveraged the existing time synchronization algorithms for radar sensing, as proposed in this paper.

III. Signal Model

In this section, we introduce the model of communication waveforms, including both the single carrier and multiple carrier cases, for embedding the sensing function.

A. Single Carrier Waveform

We consider the following waveform with a single carrier, which consists of consecutive N information symbols:

$$s(t) = \sum_{n=1}^{N} X_n(t - nT) \exp\left(j2\pi f_c t\right), \tag{1}$$

where X_n is the n-th information symbol, T is the symbol period, f_c is the carrier frequency and the phase is omitted for notational simplicity. We assume that the information symbols are mutually independent. The bandwidth of the communication signal is approximately $\frac{1}{T}$. For simplicity, we assume that Tf_c is an integer, namely each symbol period covers an integer number of carrier periods.

B. Multicarrier Waveform

We consider M subcarriers and N consecutive symbols for the case of multicarrier. The transmitted signal is given by

$$s(t) = \sum_{n=1}^{N} \sum_{m=1}^{M} X_n^m(t - nT) \exp\left(j2\pi(f_c + (m-1)\Delta_f)t\right), \tag{2}$$

where Δ_f is the frequency gap between two successive subcarriers. The bandwidth approximately equals $M\Delta_f + \frac{1}{T}$. X_n^m are assumed to be i.i.d. for different m and n.

C. Pulse Shape

In typical communication systems, a pulse shape is used to modulate the sinusoidal waveform for limited bandwidth and the removal of inter-symbol interference. Therefore, the baseband information symbol is given by $X_n(t) = x_n g(t)$, where x_n is a complex number representing the information and $g(t)$ is the pulse shape. In this paper, we will consider the rectangular and raised cosine pulse shapes, respectively.

D. Received Signal

When the signal is reflected by a stationary target, the signal received by the radar receiver is given by $r(t) = s(t - \tau) + w(t)$, where τ is the round trip time and equals $\frac{2d}{c}$, where d is the distance and c is the light speed, and w is the thermal noise. Note that the loss of signal power due to the propagation and reflection is taken into the noise power normalized by the signal-to-noise ratio (SNR).

IV. Single Carrier Sensing

In this section, we analyze the performance of typical sensing tasks, based on the single-carrier communication waveforms. Essentially, the bandwidth for sensing provided by the communication signal is achieved by the pseudo randomness of information symbol. Here the pseudo randomness is because the JCS receiver knows all the transmitted information symbols, thus being essentially deterministic.

A. Detection and Ranging: Autocorrelation Approach

If we can obtain the timing of the received signal and thus the time delay τ, we can estimate the distance d. Therefore, we can calculate the correlation between the transmitted signal, with a certain delay, and the received signal. The peak of the correlation determines the time offset between the two sequences. Meanwhile, a significant peak also indicates the existence of reflected signal and thus a significant target.

1) Decision Rules: After down-conversion from the carrier frequency, the received baseband signal is sampled with sampling period T_s. For simplicity, we assume that T is a multiple of T_s, namely $T = KT_s$. Then, it is correlated with the samples of transmitted signal having different delays:

$$R(n) = \frac{1}{KN - n} \sum_{k=n}^{KN} s((k-n)T_s) r(kT_s). \quad (3)$$

The detection of target is formulated as the following hypothesis problem:

$$decision = \begin{cases} H_1, & \max_n |R(n)| \geq \gamma \\ H_0, & \max_n |R(n)| < \gamma \end{cases}, \quad (4)$$

where γ is a preset threshold, and H_0 and H_1 mean the absence and existence of a target, respectively.

The estimation on the round trip time is then given by

$$\hat{\tau} = T_s \arg\max_n |R(n)|. \quad (5)$$

2) Gaussian Approximation: When $n = \tau$, we have

$$R(\tau) = \begin{cases} 1 + R_w(\tau), \text{ if } H_1 \\ R_w(\tau), \text{ if } H_0 \end{cases}, \quad (6)$$

where $R_w(n) = \frac{1}{N} \sum_{k=1}^{N-n} X_k^* W(k+n)$. We denote by σ_w^2 the variance of each $R_w(n)$. When $n \neq \tau$, we can approximate $R(n)$ by Gaussian distribution due to the central limit theorem:

$$R(n) \sim \begin{cases} \mathcal{N}(0, \frac{1}{N} + \sigma_w^2), \text{ if } H_1 \\ \mathcal{N}(0, \sigma_w^2), \text{ if } H_0 \end{cases}. \quad (7)$$

Moreover, we assume that the maximization operation in both (4) and (5) are confined to $s < N_1 \ll N$ values with time offset around τ, due to prior information on the distance (e.g., the target cannot be 300km away). Therefore, we can consider the N_1 autocorrelation values as independent Gaussian random variables, by ignoring their weak correlations.

3) Performance Analysis: For the performance of target detection, the missed detection probability is given by

$$\begin{aligned} p_{md} &= P(\max_s |R(s)| < \gamma | H_1) \\ &\approx P(|R(\tau)| < \gamma | H_1) \\ &= \Phi\left(\frac{\gamma - 1}{\sigma_2^2}\right) - \Phi\left(\frac{1 - \gamma}{\sigma_2^2}\right), \end{aligned} \quad (8)$$

where Φ is the cumulative distribution function (cdf) of standard normal distribution (the corresponding probability density function (pdf) is denoted by ϕ), and the false alarm rate is given by

$$\begin{aligned} p_{fa} &= P(\max_s |R(s)| > \gamma | H_0) \\ &= N_1 2^{N_1} \int_\gamma^\infty \phi\left(\frac{x}{\sigma_w^2}\right) \left(\Phi\left(\frac{x}{\sigma_w^2}\right) - \frac{1}{2}\right)^{N_1 - 1} dx. \end{aligned} \quad (9)$$

For the estimation of τ, the mean square error (MSE) is given by

$$\begin{aligned} MSE &= \frac{T^2}{12} P(\hat{\tau} = \tau) + \frac{(N_1 T)^2}{12} P(\hat{\tau} \neq \tau) \\ &= \frac{(N_1 - 1) T^2 2^{N_1 - 1}}{12} \int_0^\infty \int_0^x \phi\left(\frac{x-1}{\sigma_w^2}\right) \phi\left(\frac{y}{\sigma_w^2}\right) \\ &\times \left(\Phi\left(\frac{y}{\sigma_w^2}\right) - \frac{1}{2}\right)^{N_1 - 1} dxdy \\ &+ \frac{(N_1 - 1)^3 T^2 2^{N_1 - 1}}{12} \int_0^\infty \int_x^\infty \phi\left(\frac{x-1}{\sigma_w^2}\right) \phi\left(\frac{y}{\sigma_w^2}\right) \\ &\times \left(\Phi\left(\frac{y}{\sigma_w^2}\right) - \frac{1}{2}\right)^{N_1 - 1} dxdy, \end{aligned} \quad (10)$$

where the second term dominates the MSE.

B. Detection and Ranging: Time Synchronization

The above autocorrelation-based approach is essentially time synchronization using the known data as pseudorandom sequence. The major challenge is the computational cost and delay, since the autocorrelation function needs to be computed from sufficiently many information symbols. An alternative approach is to leverage existing algorithms of time synchronization in communication systems. In this paper, we consider the celebrated Early-Late Gate Timing algorithm [20]. Other time synchronization algorithms such as the Gardner's algorithm [19] can also be applied.

The Early-Late Gate Timing algorithm [20] is briefed as follows. First we assume that a coarse timing information has been obtained, namely the synchronization has been fixed to the scale of one information symbol. This can be achieved by coarse sampling and correlation analysis. Suppose that, in the n-th information symbol, three samples are made at time $\tau_n - \delta$, τ_n and $\tau_n + \delta$, respectively, where τ_n is the center sample time and is adjustable in different information symbols while δ is fixed. The timing discriminating function $m(n, \tau_n)$ is computed by $m(n, \tau_n) = x_n X_n^*(\tau_n + \delta) - x_n X_n^*(\tau_n - \delta)$. Then, the sampling time τ_n is changed by

$$\tau_{n+1} = \tau_n + \gamma m(n, \tau_n), \quad (11)$$

where γ is the step size. The convergence implies the time synchronization.

V. Multicarrier Sensing

In this section, we focus on the multicarrier case, which leverages the fine timing structure of wideband signals.

A. Ranging Algorithm

For the ranging task, we use the analysis in the frequency domain. For Gaussian noise, the n-th received symbol modulated on the m-th subcarrier is given by the maximum likelihood estimation:

$$\tilde{X}_n^m = X_n^m e^{-j2\pi(m-1)\Delta_f \tau} + W_n^m, \quad (12)$$

where X_n^m is the transmitted baseband symbol, W is the white Gaussian noise and the extra phase $2\pi(m-1)\Delta_f\tau$ is due to the round trip time τ. Note that the noise power has been normalized for the proper SNR. Collecting the observations on all the M carriers and N symbol periods, the maximum likelihood (ML) estimation of the round trip time is given by

$$\tau = \min_t \sum_{m=1}^{M}\sum_{n=1}^{N} \left\| \tilde{X}_n^m - X_n^m e^{-j(m-1)\Delta_f t} \right\|^2. \quad (13)$$

Note that $\tilde{X}_n^m$ is obtained from the measurements, and X_n^m is known in advance. The only unknown is the time delay τ.

Taking the derivative of the targetive function in (13) to be zero, we have

$$\sum_{m=1}^{M}\sum_{n=1}^{N} \Im[\Theta_{mn}(t)] = 0 \quad (14)$$

where $\Im[\Theta_{mn}(t)] = \frac{d}{dt}\left\| \tilde{X}_n^m - X_n^m e^{-j(m-1)\Delta_f t} \right\|^2$, and $\Theta_{mn}(t)$ is given by

$$\begin{aligned} \Theta_{mn}(t) &= -2(m-1)\Delta_f \tilde{X}_n^{m*} X_n^m e^{-j(m-1)\Delta_f t} \\ &= -2(m-1)\Delta_f \mathbf{1}^T(\mathbf{A}\odot\mathbf{X}\odot\tilde{\mathbf{X}})\mathbf{1}, \end{aligned} \quad (15)$$

where $\mathbf{A}_{mn} = e^{-j(m-1)\Delta_f t}$, $\mathbf{X} = (X_{mn})_{mn}$, $\tilde{\mathbf{X}} = (\tilde{X}_{mn})_{mn}$ and $\odot$ is the Hadamard product.

For minimizing the targetive function in (13), we can carry out the gradient descent iterations, namely

$$t^{k+1} = t^k - \gamma_t \sum_{m=1}^{M}\sum_{n=1}^{N} \Im[\Theta_{mn}(t^k)]. \quad (16)$$

The corresponding physical meaning in the iteration in (16) is intuitive, which is similar to that of phase lock loop (PLL).

However, the gradient descent approach in (16) faces the challenge of local minimum. The target function in (13) is shown in Fig. 2 for the case of 160MHz bandwidth. We observe that, if the initial distance error is beyond a few meters, the gradient search will stop at a local minimum. The local minima will be significant if the total bandwidth is large. The major reason is that, when $m\Delta_f$ is large, the phase $\Delta_f(t-t_0)$ will be more than 2π, thus reversing the leading and lagging roles of X and $\tilde{X}$ and directing t to an opposite direction.

To handle the challenge of local minima, a simpler line search for the optimum in (13) can be adopted, since t is 1-dimensional, and the range of distance (thus the searching range of t) can be determined in advance.

VI. Performance Trade-off

In this section, we analyze the performance trade-off between communications and radar sensing. For simplicity,

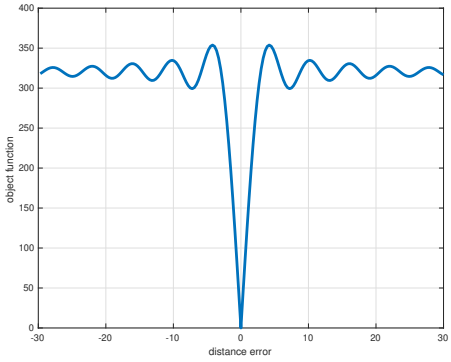

Fig. 2: The target function in (13) when $M = 512$ and $\Delta_f = 312.5kHz$, in the noise-free case

we consider the single-carrier case and assume the pulse amplitude modulation (PAM) with S levels. Note that QAM is simply the combination of PAMs over the in-phase and quadrature branches.

The performance metric for ranging in (10) is difficult to analyze, since it concerns the detailed algorithms. Therefore, we have the following Cramer-Rao bound:

Proposition 1. *For the single-carrier JCS with S-PAM and transmit powers $\{P_s\}_{s=1,\ldots,S}$, the Cramer-Rao bound satisfies*

$$\textit{C-R bound} \propto \sum_{s=1}^{S}\frac{1}{P_s} \geq \frac{S}{\sum_{s=1}^{S} P_s}, \quad (17)$$

where the inequality is based on the harmonic-arithmetic mean inequality, and the equality holds for equal P_s's.

The proposition implies that, for radar ranging, it be desirable to arrange identical power to different symbols. However, communications need to set statistically different powers for different symbols (otherwise, no information can be conveyed). From the viewpoint of information theory, the (real) signal amplitude distribution should be Gaussian distributed, in order to maximize the channel capacity. Therefore, communications and radar conflict in the power of different symbols. One possible solution is to use phase shift keying (PSK), which has a constant symbol power; however, it has less spectral efficiency compared with QAM for communications.

Letting $S \to \infty$ and the probability density function (PDF) of signal amplitude is denoted by p_t. Then, we quantize the trade-off between communications and radar sensing in the following two regrets:

- Communication regret (i.e., the channel capacity loss):

$$regret_c = \log(P+\sigma_n^2) - h(Y) = D(f||g) \quad (18)$$

TABLE I: Configuration of single carrier JCS

distance	100m	symbol duration T	0.1us
Pulse β	0.2	modulation	16QAM
Sampling rate	100Msps	SNR	-20dB

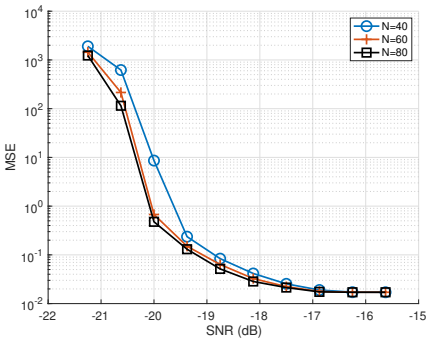

Fig. 3: MSE of ranging using correlation analysis (single carrier)

where Y is the received signal, X satisfies the distribution p_t, h is the differential entropy, f (depending on p_t) and g are the distribution of Y and Gaussian distribution, respectively, both having variance $P+\sigma_n^2$, and D is the Kullback-Leibler distance.

- Radar regret (i.e., the gap of the Cramer-Rao bound):

$$regret_r = \frac{1}{P} - \int_{-\infty}^{\infty} \frac{p_t(x)}{x^2} dx, \tag{19}$$

where satisfies $P = \int_{-\infty}^{\infty} p_t(x)x^2 dx$.

Therefore, the trade-off of communications and sensing in JCS is characterized by the gap to Gaussian distribution and the gap of harmonic mean and arithmetic mean.

VII. Numerical Simulations

In this section, we provide the numerical simulation results.

A. Single Carrier

We first consider the case of single carrier. The setups for the system are given in Table I, unless mentioned otherwise.

1) Sensing Performance: We first show the performance of sensing, while the communication data rate is 40Mbps in the standard setup. Fig. 3 shows the MSE of ranging, using the autocorrelation analysis with respective to different numbers of information symbols and different SNRs. We observe that the standard deviation of ranging error drops below 1m when the SNR is above -20dB. Moreover, when N is increased, the more precise estimation of autocorrelation function yields a better performance of ranging.

Fig. 4 shows the performance of the early-late gate time synchronization based ranging with respective to different raised cosine pulse shapes (namely different β's) and different

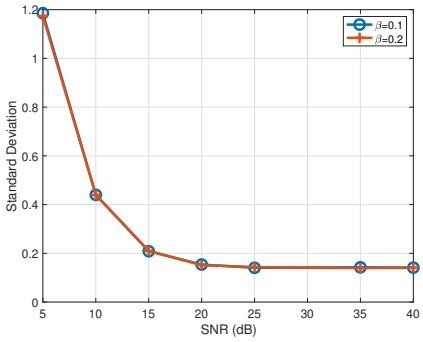

Fig. 4: MSE of ranging using early-late time synchronization (single carrier)

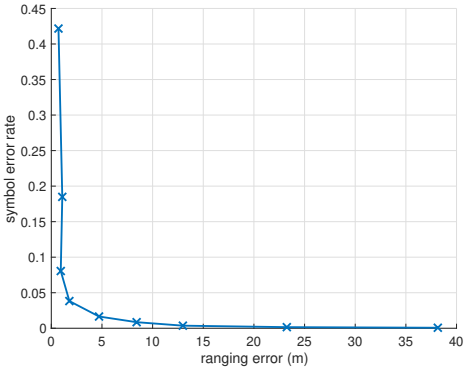

Fig. 5: Trade-off between communications and radar (single carrier)

SNRs. We observe that the standard deviation is below 1 meters only when the SNR is more than 5dB, which is much higher than that of the autocorrelation analysis. We further observe that the different values of β in the raised cosine pulse shape do not impact the performance. A further observation is that the performance of the early-late gate algorithm drops radically when SNR decrease, which implies that this algorithm be suitable for high-SNR scenarios.

2) Communication-Sensing trade-off: The trade-off between communications and radar ranging, in the single carrier case, is shown in Fig. 5. In the simulation, we assume the power spectral density of noise to be -174dBm/Hz and the transmit power is 20mW. We assume a path loss factor of 3.5 and a distance of 100m. We consider the trade-off due to the reflection, where the portion of reflected power ranges between 0.1 and 0.9 (thus the performance of communications decreases while that of radar is improved). In Fig. 5, we observe a clear trade-off between communications and ranging. In particular, we observe that the trade-off curve mainly consists of two straight lines, while the transience is very short. The rapid change of the trade-off curve is due to the waterfall phenomenon of the ranging performance,

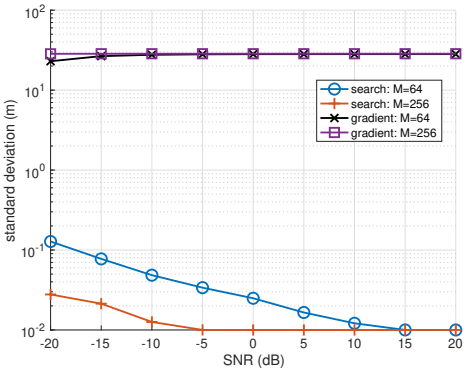

Fig. 6: Performance of multicarrier ranging

namely the performance of ranging quickly deteriorates when the noise power is above a threshold. Therefore, unless being in the short transience period, the performance of ranging is almost constant (either good or very bad), almost regardless of the communication performance.

B. Multiple Carriers

Now, we study the case of multiple carriers. The ranging performance of multiple carriers, based on the line searching and gradient descent approaches, is shown in Fig. 6. Note that we add a 0.01m floor for the ranging error. The algorithms are tested for the cases of 64 and 256 carriers, each of which occupies a 312.5kHz bandwidth (by following the parameters of IEEE 802.11g). We observe that the performance of the line search achieves a much better performance, where the ranging error decreases with the SNR. In a contrast, the gradient descent approach incurs substantial error due to the local minimum problem. Although stochastic gradient approach can help to alleviate the local minimum problem, it is a better choice to use the simple and efficient line searching approach. An interesting observation is that the performance of the gradient descent is improved when the received signal is more noisy. A possible explanation is that the random noise helps to leave the local minima, similarly to the random perturbation in stochastic gradient algorithms.

VIII. Conclusions

In this paper, we have studied the JCS using traditional communication waveforms. We have studied both cases of single carrier and multiple carriers. For the single carrier case, we have considered the autocorrelation and time synchronization approaches for identifying the timing information; for the case of multiple carriers, we have used the ML estimation of timing with either gradient search or line search. The trade-off of communications and sensing in JCS is characterized by the regrets of both functions with respect to the optimal performances. Finally, numerical simulations have been carried out the validate the proposed algorithms and analyses.

References

[1] H. He, J. Li and P. Stoica, *Waveform Design for Active Sensing Systems: A Computational Approach*, Cambridge University Press, 2012.

[2] F. Lemic, J. Martin, C. Yarp, D. Chan, V. Handziski, R. Rroderson, G. Fettweis, A. WOlisz and J. Wawrzynek, "Localization as a feature of mmWave communication," in *Proc. of International Wireless Communications and Mobile Computing Conference (IWCMC)*, 2016.

[3] M. Alloulah and H. Huang, "Future millimeter wave indoor systems: A blueprint for joint communication and sensing," *Computers*, vol. 52, no.7, 2019.

[4] T. Wei and X. Zhang, "mTrack: High-precision passive tracking using millimeter wave radios," in *Proc. of ACM MobiCom*, 2015.

[5] S. Prasad, M. T. Panigrahi, M. Hassan, "Direction of arrival and center frequency estimation for impulsive radio millimeter wave communications," in *Proc. of ACM mmNets*, 2018.

[6] H. S. Ghadikolaei, H. Ghauch and C. Fischione, "Learning-based tracking of AoAs and AoDs in mmWave networks," in *Proc. of ACM mmNets*, 2018.

[7] J. Lie, N. Gillian, M. E. Karagozler, P. Amihood, C. Schwesig and E. Olson, "Soli: Ubiquitous gesture sensing with millimeter wave radar," in *Proc. of SIGGRAPH*, 2016.

[8] C. Xu, Z. Li, H. Zhang, A. S. Rathore, H. Li, C. Song, K. Wang and W. Xu, "WaveEar: Exploring an mmWave-based noise-resistant speech sensing for voice-user interface," in *Proc. of ACM MobiSys*, 2019.

[9] Z. Li, B. Chen, H. Li, C. Xu, X. Chen, K. Wang, W. Xu, "FerroTag: A Paper-based mmWave-Scannable Tagging Infrastructure", in *ACM International Conference on Sensor Networked Systems (SenSys)*, 2019

[10] Z. Li, Z. Yang, C. Song, Z. Peng, C. Li, W. Xu, "E-Eye: Hidden Electronics Recognition through mmWave Nonlinear Effects", in *Proc. of ACM International Conference on Sensor Networked Systems (SenSys)*, 2018

[11] K. Qian, C. Wu, Z. Yang, Y. Liu and K. Jamieson, "Widar: Decimeter-level passive tracking via velocity monitoring with commodity Wi-Fi," in *Proc. of ACM Mobihoc*, 2017.

[12] D. Vasisht, S. Kumar and D. Katabi, "Decimeter-Level Localization with a Single WiFi Access Point," *ACM NDSI*, 2016.

[13] N. J. Willis, *Bistatic Radar*, Artech House, 1991.

[14] M. Radmard, M. Bastani, F. Behnia, "Advantage of the DVB-T signal for passive radar applications," in *Proc. of International Radar Symposium*, 2010.

[15] E. Glennon, A. Dempster and C. Rizos, "Feasibility of air target detection using GPS as a bistatic radar," *Global Positioning System*, vol. 5, no.1, pp.119–126, 2006.

[16] J. Bai, J. Wang, "Weak target detection using dynamic programming TBD in CDMA based passive radar," in *Proc. of IET International Radar Conference*, 2009.

[17] L. Yujiri, M. Shoucri and P. Moffa, "Passive millimeter-wave imaging," *IEEE Microwave Magazine*, vol.47 no.9, pp.39–50, 2003

[18] Y. Meng, A. Qing, C. Lin, J. Zang, Y. Zhao and C. Zhang, "Passive millimeter wave imaging system based on helical scanning," *Scientific Reports*, vol.8, 2018.

[19] F. M. Gardner, "A BPSK/QPSK timing-error detector for sampled receivers," *IEEE Trans. on Comm.*, vol.34, no.5, pp.423-429, 1986.

[20] F. Ling, *Synchronization in Digital Communication Systems*, Cambridge University Press, 2017.

[21] A. Evers and J. A. Jackson, "Analysis of an LTE waveform for radar applications," in *Proc. of IEEE Radar Conference*, 2014.

[22] Y. Fan, J. Bao, M. S. L. Aljumaily, and H. Li, "Communications via frequency-modulated continuous-wave radar in millimeter wave band," in *IEEE International Global Communications Conference,* 2019.